



Journal of Mining and Environment (JME)

journal homepage: www.jme.shahroodut.ac.ir



Prediction of Acid Mine Drainage Generation Potential of A Copper Mine Tailings Using Gene Expression Programming-A Case Study

Behshad Jodeiri Shokri^{1*}, Hessam Dehghani¹, Reza Shamsi¹ and Faramarz Doulati Ardejani²

1. Department of Mining Engineering, Hamedan University of Technology, Hamedan, Iran

2. School of Mining, College of Engineering, University of Tehran, Tehran, Iran

Article Info

Received 31 August 2020

Received in Revised form 21 October 2020

Accepted 2 November 2020

Published online 2 November 2020

DOI:10.22044/jme.2020.10031.1938

Keywords

Acid mine drainage

Copper tailing

Pyrite

Chalcopyrite

Gene expression programming

Abstract

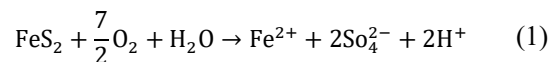
This work presents a quantitative predicting likely acid mine drainage (AMD) generation process throughout tailing particles resulting from the Sarcheshmeh copper mine in the south of Iran. Indeed, four predictive relationships for the remaining pyrite fraction, remaining chalcopyrite fraction, sulfate concentration, and pH have been suggested by applying the gene expression programming (GEP) algorithms. For this, after gathering an appropriate database, some of the most significant parameters such as the tailing particle depths, initial remaining pyrite and chalcopyrite fractions, and concentrations of bicarbonate, nitrite, nitrate, and chloride are considered as the input data. Then 30% of the data is chosen as the training data randomly, while the validation data is included in 70% of the dataset. Subsequently, the relationships are proposed using GEP. The high values of correlation coefficients (0.92, 0.91, 0.86, and 0.89) as well as the low values of RMS errors (0.140, 0.014, 150.301, and 0.543) for the remaining pyrite fraction, remaining chalcopyrite fraction, sulfate concentration, and pH prove that these relationships can be successfully validated. The results obtained also reveal that GEP can be applied as a new-fangled method in order to predict the AMD generation process.

1. Introduction

Tailings and wastes, which result from the mining activities, are the most abundant volumes of solid materials worldwide. Some of the most significant environmental problems caused by these wastes and tailings at the global scale include the generation of acid mine drainage (AMD) and the pollutions resulting from the high concentration of dissolved metals in underground and surface water bodies. AMD is generated where the sulfidic minerals in mining sites are exposed to water and atmospheric oxygen. The AMD generation would be considered as a concern wherever the sulfate minerals (mainly pyrite, chalcopyrite) exist and the pH has low values [1].

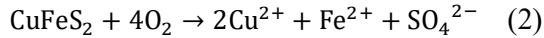
Several critical factors affect the pyrite and chalcopyrite oxidation processes, as follow: the presence of oxygen, ferric iron, temperature, presence/absence of microorganisms, Eh, and pH. Indeed, the mentioned parameters play essential

roles in opting further reclamation and treatment strategies or even in selecting the mineral processing methods, motivating the researchers toward performing a vast array of studies on relevant topics during these recent decades [2-5]. Reaction (1) expresses the most crucial pyrite oxidation reaction in the presence of oxygen, which leads to the formation of AMD:

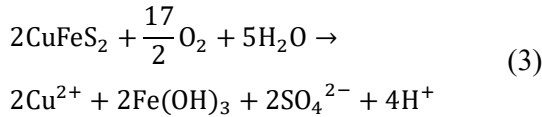


As it can be seen, the products of this oxidation reaction are ferrous iron, sulfate, and acid, which would be considered as the output parameters including the remaining pyrite fraction, sulfate, and pH in this research work. Moreover, a complete oxidation of chalcopyrite (CuFeS_2), which leads to the generation of AMD, is presented as follows (reaction 2) [6]:

✉ Corresponding author: b.jodeiri@hut.ac.ir (B. Jodeiri Shokri).



As it can be seen in reaction (2), the complete oxidation of chalcopyrite ends up producing no acid product. Nevertheless, a combination of the oxidation process of the ferrous iron and iron hydroxyl is known to regenerate the acid (reaction (3)).



Rimsdith *et al.* (1994) have found that chalcopyrite oxidation accelerates with rising the ferric iron concentration. The increase is, however, lower than that for the pyrite by 1 to 2 folds [6].

Ferguson and Erickson (1988) have described that the factors controlling the AMD formation are generally characterized in three affectors: (a) primary, (b) secondary, and (c) tertiary. The parameters involved in acid production are considered as the primary parameters [7]. The second factors are those responsible for controlling the consumption of the products triggering the acid reactions. The third factors are related to the physical characteristics of the waste particles that can directly affect acid production, transportation, and consumption. Indeed, these three different factors have major roles in the AMD reactions and the quality of proceeding water from the waste particles.

During the past 50 years, many research works have targeted the environmental issues of sulfide mineral oxidation and associated AMD or what is generally referred to as acid rock drainage (ARD) alongside the processes through which the metals and those minerals are dissolved or precipitated. Accordingly, the researchers have long tried to use the experimental methods (e.g. static and kinetic tests) along with the numerical, stochastic, and even intelligent methods to estimate the parameters affecting the AMD generation. For instance, Rooki *et al.* (2011) have managed to predict the heavy metals of copper, iron, magnesium, and zinc in AMD using the back-propagation neural networks (BPNN), general regression neural networks (GRNN), and multiple linear regression (MLR). The results obtained proved that BPNN and GRNN could serve as appropriate techniques for a quick and cost-effective estimation of the heavy metals resulting from AMD [8]. Aryafar *et al.* (2012) have predicted the concentrations of heavy metals triggered by AMD by applying the support vector machine (SVM) techniques. They further

compared the results obtained with those of GRNN. The results showed a higher accuracy and a faster pace of SVM, as compared with GRNN in this case [9]. Doulati Ardejani *et al.* (2012) have used GRNN to predict the concentrations of REEs resulting from neutral alkaline mine drainage (NAMD) at the Razi coal mine in the north of Iran. The NAMD case was characterized by low concentrations of REEs, high concentrations of sulfate, and bicarbonate, while the pH value was almost 9. In order to verify the GRNN technique, its results were compared with those of MLR, which showed that GRNN could be more reliable than MLR [10]. Sadeghimirshahidi *et al.* (2013) have applied ANN to estimate the pyrite fractions within a coal pile. For this purpose, they considered different input parameters including the depth of the pile, initial pyrite fraction, diffused oxygen fraction throughout the wastes, and annual precipitation data [11]. Bouzahzah *et al.* (2014) have compared the static test with different mineralogical contents to evaluate the significance of mineralogical studies in AMD prediction. A modified kinetic test was compared with the standard kinetic test protocol in this research work [12]. Jodeiri Shokri *et al.* (2014a) used an adaptive neuro-fuzzy inference system (ANFIS) method to evaluate the pyrite contents within an abandoned coal waste pile. They found that their hybrid method, ANFIS, had better results than the ANN results [13]. In another research work on the same case, Jodeiri Shokri *et al.* (2014b) have presented a statistical relationship for estimating the pyrite contents. In 2016, Bahrami and Doulati Ardejani estimated the oxidation of the pyrite process using an ANN-simulated annealing (SA) hybrid method. They concluded that the results obtained from SA provided a better estimation than either ANN or the statistical method [15]. Dold (2017) has reviewed all the predicting techniques in AMD prediction. His critical review highlighted the ARD prediction based on the involvement of geochemical processes [16]. Balci and Demirel (2018) have used acid base accounting (ABA), aqueous leaching, and net acid generation (NAG) tests and mineralogical studies in order to predict AMD resulting from the largest historical copper deposits of Turkey [17]. Hadadi *et al.* (2020) have applied a probabilistic approach to predict how acid mine drainage is generated within coal waste particles. After building a dataset with historical data of an abandoned pile, they considered some parameters such as the depth of the waste, concentration of bicarbonate, and oxygen fraction as the input data, while the remaining pyrite fraction was the output

data. Then the best distribution functions were determined using the Monte Carlo simulation. Subsequently, the best probability distribution functions of the input parameters were inserted into the linear statistical relationships to find the probability distribution function of the output data [18].

Nevertheless, many treatment techniques have been developed for reducing and neutralizing the AMD issues during these years. For instance, Sebogodi *et al.* (2019) have used green liquor dregs from two Kraft pulp manufactures in South Africa [19]. In another research work, a pilot-scale of the operational conditions of the actual AMD nanofiltration (NF) was used by Luis *et al.* (2020). Indeed, this method was applied to recover water that could be used as a tool for copper recovery [20]. Zhou *et al.* (2020) have proposed an index system of surface mining based on safety, high efficiency, and environmental influence [21]. Chen *et al.* (2020) have suggested another evaluation index for green mine construction based on Driver–Pressure–State–Impact–Response (DPSIR) [22].

Along with these artificial intelligence (AI) techniques, gene expression programming (GEP) has intensively been applied in different scopes of mining engineering. For instance, Behnia and Shariar (2015) have used GEP to predict the tunnel-induced settlement [23]. In 2015, Johari and Hoshmand Nejad applied GEP to predict the soil-water characteristic curve [24]. Shirani Faradonbeh *et al.* (2018) have estimated an environmental issue resulting from blasting using GEP and GP. For this purpose, they collected 92 blasting events, and subsequently, they measured air overpressure (AOp). The results obtained revealed that GEP had a precise estimation than the other models [25]. Thneibat and Tarawneh (2019) have applied GEP to select the appropriate ground improvement technique by increasing the soil bearing capacity, reducing potential settlement, and mitigating liquefaction [26]. Hajihassani *et al.* (2019) have presented an equation by the GEP algorithm to predict the convergence of tunnels [27].

It should be noted that the mathematical relationships governing the pyrite and chalcopyrite oxidation processes and their subsequent products are too complicated and their solutions are time- and cost-consuming. Indeed, the primary motivation leading various researchers toward using the statistical and intelligent methods has been to formulate simple yet high-accuracy mathematical equations. The literature review also revealed that some of the applied intelligent algorithms had better results than the conventional

methods. Also the literature review showed that the GEP algorithm was not applied in predicting the AMD formation. For this purpose, the present research work is an attempt to apply the GEP algorithm to suggest relationships to predict the remaining pyrite fraction and chalcopyrite fraction through the tailings at the Sarcheshmeh copper mine in the south of Iran.

1.2. Site Description

The Sarcheshmeh copper mine is situated 50 km to the south of Rafsanjan in the central part of Zagros Mountain Range. It supplies one of the largest mining complexes in the Middle East. The geological reserve of the mine has been estimated to exceed 1.2 billion tons of sulfuric copper ore with an average grade of 0.7%. In terms of geology, the Sarcheshmeh copper mine was formed on the global copper belt, covering a large 1200×2300 m ellipsoidal area from the SE to the NW with an average ore depth of 1612 m.

The mine is located in a region that is categorized as a cold desert climate. The average precipitation in the area is around 550 mm per year. The temperature varies from -15° in the winter to $+32^\circ$ in the summer. The dumps are covered by snow for three to four months per year. Based on the field observations and previous research works, mineral processing operations result in the production of more than 24 megatons of tailing over an area of more than 4 km² within the studied area. In some cases, the dump height reaches 12 m [28].

2. Materials and Methods

2.1. An overview of GEP algorithm

GEP is based on the evolutionary computations inspired by the natural evolution phenomena. This method was coined by Ferreira in 1999 and officially released in 2001 [29]. GEP integrated the ideas of the two preceding legacy algorithms including GA and GP in an attempt to cover their shortcomings. In this methodology, the genotype of the chromosomes possesses a linear structure, similar to the case with GA. On the other hand, the phenotype of the chromosomes exhibits a tree structure with variable length and size, similar to the case with genetic programming (GP). Karva code is the language of choice for GEP, and multiple genes are used to capture the multiple structures of chromosomes and the ability to generate subtrees, providing the algorithm with a better compatibility and performance [30]. According to the flowchart of GEP (Figure 1), the beginning of the algorithm is random with the

generation of an initial population. The generated chromosomes are then expressed followed by evaluating each individual based on an evaluation function with a selection process then performed based on the evaluation results. Applying particular modifications to the selected individuals, a new population of the selected individuals with new characteristics is generated. The new population will then repeat the mentioned procedure, and this process continues until an appropriate solution is achieved (Figure 1) [28].

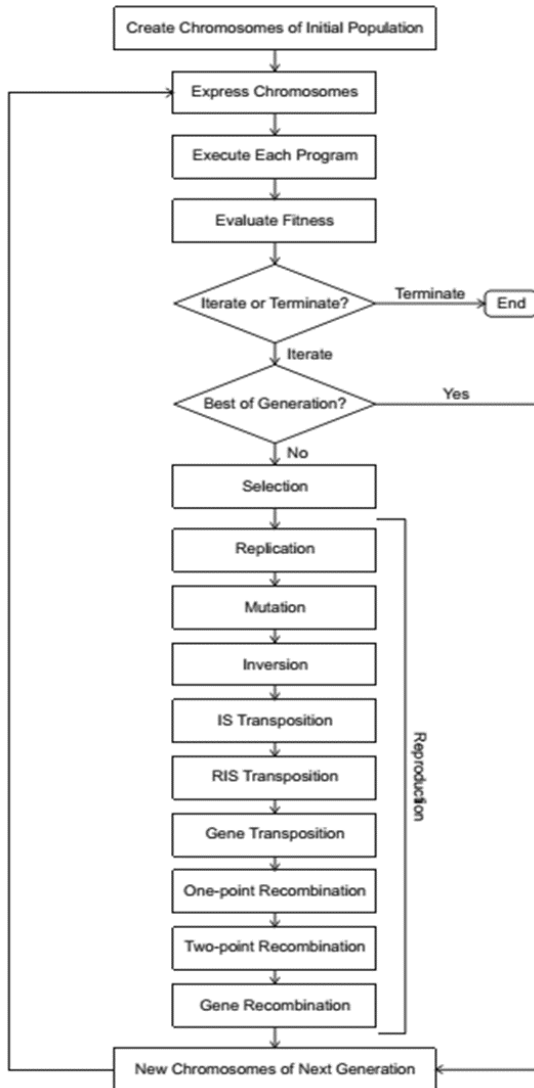


Figure 1. Flowcharts of GEP.

2.2. Open reading frames and genes

The open reading frames (ORFs) can help to better understand GEP. From the biological viewpoint, a coding gene sequence begins with the “start”codon. Then it continues with the amino acid codons, and the termination codon is the ending

point [29]. It should be noted that the start point is generally considered the first position of a gene, while the termination point may not always be with the last position of a gene. The non-coding region downstream from the termination point is usual in genes. An algebraic example is given for a better understanding of the expression (Equation 4) [29]:

$$\sqrt{(a + b) \times (c - d)} \tag{4}$$

which can also be represented as a diagram or ET, as follows (Figure 2) [29]:

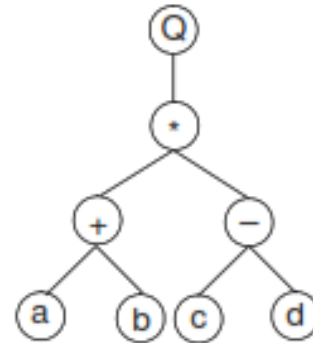


Figure 2. An ET example.

The square root function is presented by “Q”. This kind of diagram representation is in fact the phenotype of GEP individuals, being the genotype easily inferred from the phenotype as follows:

The ET reads from left to right and from top to bottom.

2.3. Gene expression programming genes

Head and tail are the main parts of the GEP genes. Although the head is composed of the function set F and the terminal set T, the tail has only terminals. As a result, there are two different alphabets at various regions within a gene. The length of each head is selected whereas the length of tail t is defined by a function of h (Equation 5) [29]:

$$t = h(n_{max} - 1) + 1 \tag{5}$$

In this equation, n is the number of arguments of the function.

Suppose that you have a gene as {Q, *, /, -, +, a, b}. In this case, n is 2. For instance, for h = 10 and t = 11, the length of the gene would be h+t, i.e. 21. Figure 3 shows this gene (the bold is tail in the figure), and as a consequence, ET will be coded as follows [29]:

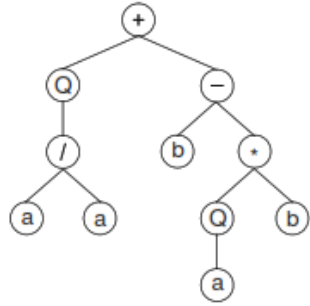


Figure 3. An ET example for describing head and tail

2.4. Fitness Function

The first step of the GEP algorithm is the choice of a fitness function. In this work, Equation (6) was considered as the fitness function.

$$RMSE = \sqrt{\frac{1}{n} \sum_{i=1}^n (P_i - O_i)^2} \tag{6}$$

where:

n: number of data points;

P_i: estimated data;

O_i: real data.

3. Results and Discussions

3.1. Dataset

As mentioned earlier, the AMD generation was predicted by applying the gene expression programming algorithm. For this purpose, all the experimental data was collected from the tailing dumps in the previous studies such as Jannesar Malakooti *et al.* (2014), which was gathered to build a database. A brief database is presented in Table 1. Then the input and output data was selected according to the available data. The depth of the tailings within the dump, fraction of diffused oxygen through the waste particles, concentrations of bicarbonate, chloride, nitrite, and nitrate, initial pyrite, and chalcopyrite fractions within the dump were considered the as input data. Moreover, the remaining pyrite fraction, the remaining chalcopyrite fraction, and pH values were selected as the output data. Then the GEP algorithm was used to find the best relationships between each output and all the inputs. The range of the input and output parameters is listed in Table 2. The dataset was divided into two parts: training dataset and validation dataset being made up of 70% and 30% of the database, respectively. The validation dataset was chosen randomly.

Table 1. Database of Sarcheshmeh copper tailings dump [28]

No.	Depth of tailings (m)	Bicarbonate (mg/L)	Chloride (mg/L)	Nitrite (mg/L)	Nitrate (mg/L)	Remaining pyrite fraction (%)	Remaining chalcopyrite fraction (%)	Sulfate (mg/L)	pH value
1	0.3	0	42.4	19.8	4.3	1.403	0.06	844	2.9
2	0.6	0	40.7	11	3.2	1.442	0.086	1150	3.1
3	0.9	0	34.1	12.2	1.8	1.549	0.112	1300	4.5
4	1.2	0	30.7	10.2	3.1	1.606	0.129	928	4.7
5	1.5	20	19	14.9	3.9	1.715	0.133	901	5.6
6	1.8	25	22.4	16.9	4.3	1.830	0.134	870	6.7
7	2.1	30	19	14.3	5.2	1.920	0.134	863	7
8	2.4	25	17.1	14.7	5.5	1.930	0.135	808	7.8
9	2.7	30	17.2	20.3	7.2	1.930	0.135	850	7.3
10	3	22	15.5	10.6	7.6	1.950	0.13	835	7.6
11	3.3	28	15.5	6.9	6.5	1.945	0.136	800	7.8
12	3.6	26	12.1	6.7	6.3	1.936	0.131	915	8.2
13	3.9	25	13.8	6.3	5.9	1.927	0.137	905	7.9
...
57	0.3	52.5	80.82	0.075	7.13	1.629	0.049	321.9	4.2
58	0.6	0	78.72	0.15	0	1.762	0.069	589.5	3.8
59	0.9	0	78.78	0.075	0	1.841	0.085	837	3
60	1.2	42	73.99	0.075	0	2.013	0.12	622.5	6.2
61	1.5	52.5	67.82	0.075	0	2.163	0.14	444.7	7.4
62	1.8	42	28.61	0.075	0	2.343	0.163	351.4	8.1
63	2.1	42	25.76	0.05	0	2.483	0.177	365.2	8.6
64	2.4	47.2	22.61	0.075	0	2.663	0.185	309.2	8.4
65	2.7	42	18.09	0.075	0	2.708	0.186	337.2	8.4
66	3	52.5	18.09	0.15	0	2.727	0.192	351.4	8.3
67	3.3	47.2	18.09	0.075	0	2.78	0.2	358.9	8.3
68	3.6	46.2	18.09	0.075	0	2.858	0.204	366.8	7.9
69	3.9	52.5	18.09	0.075	0	2.893	0.208	314	8.1
70	4.2	52.5	22.61	0.1	0	2.914	0.208	371.6	8

Table 2. Range of the datasets used for GEP.

Parameter	Symbol	Change interval	Type of parameter
Depth of tailings (m)	D	0.3-4.200	
Bicarbonate concentration (mg/L)	Bi	0-52.500	
Choloride concentration (mg/L)	CL	12.100-82.210	
Nitrite (mg/L)	N	0-21.700	
Nitrate (mg/L)	NN	0-22.630	
Initial remaining pyrite fraction (%)	IPy	1.950-3.159	Input
Initial remaining chalcopyrite fraction (%)	IChPy	0.137-0.261	
Remaining pyrite fraction (%)	Py	1.403-3.159	
Remaining chalcopyrite fraction (%)	ChPy	0.0094-0.261	Output
Sulfate (mg/L)	S	309.200-1960.900	
pH	pH	2.900-8.600	

3.2. GEP results

In the present work, GEP was implemented in the GeneXproTools 5.0 in order to obtain a final relationship between the input and output parameters. For this, after determining the fitness function, the next step is to select a set of functions for forming the chromosomes. According to Table 3, the most appropriate function for obtaining the

final equation for each output parameter was determined.

In the next stage, the chromosome structure, linking function, and coefficients of the genetic operators were selected. Table 4 reports the parameters used in GEP.

Figures 4 to 7 demonstrate the final equations for using the GEP algorithm in order to estimate the output parameters in the form of expression trees.

Table 3. Functions utilized in this work.

Parameter	Functions
Py	+, -, ×, ÷, exp(x), ln(x), 1/x, x ² , x ³ , $\sqrt[3]{x}$, tanh(x), (1-x)
Chpy	+, -, ×, ÷, sqrt(x), exp(x), ln(x), 1/x, x ² , x ³ , $\sqrt[3]{x}$, tanh(x), (1-x)
S	+, -, ×, ÷, sqrt(x), exp(x), ln(x), 1/x, x ² , x ³ , $\sqrt[3]{x}$
pH	+, -, ×, ÷, exp(x), ln(x), 1/x, x ² , x ³ , $\sqrt[3]{x}$, tanh(x), (1-x)

Table 4. Parameters of GEP.

Parameter	Value			
	Py	Chpy	S	pH
Number of chromosomes	34	35	37	33
Head size	7	7	7	7
Tail size	8	8	8	8
Gene size	15	15	15	15
Number of genes	4	4	4	4
Linking function	Multiplication	Multiplication	Multiplication	Multiplication
Fitness function	RMSE	RMSE	RMSE	RMSE
Mutation rate	0.008	0.07	0.01	0.06
Training	70 %	70 %	70 %	70 %
Validation	30 %	30 %	30 %	30 %
Number of generations	3000	3000	3000	3000

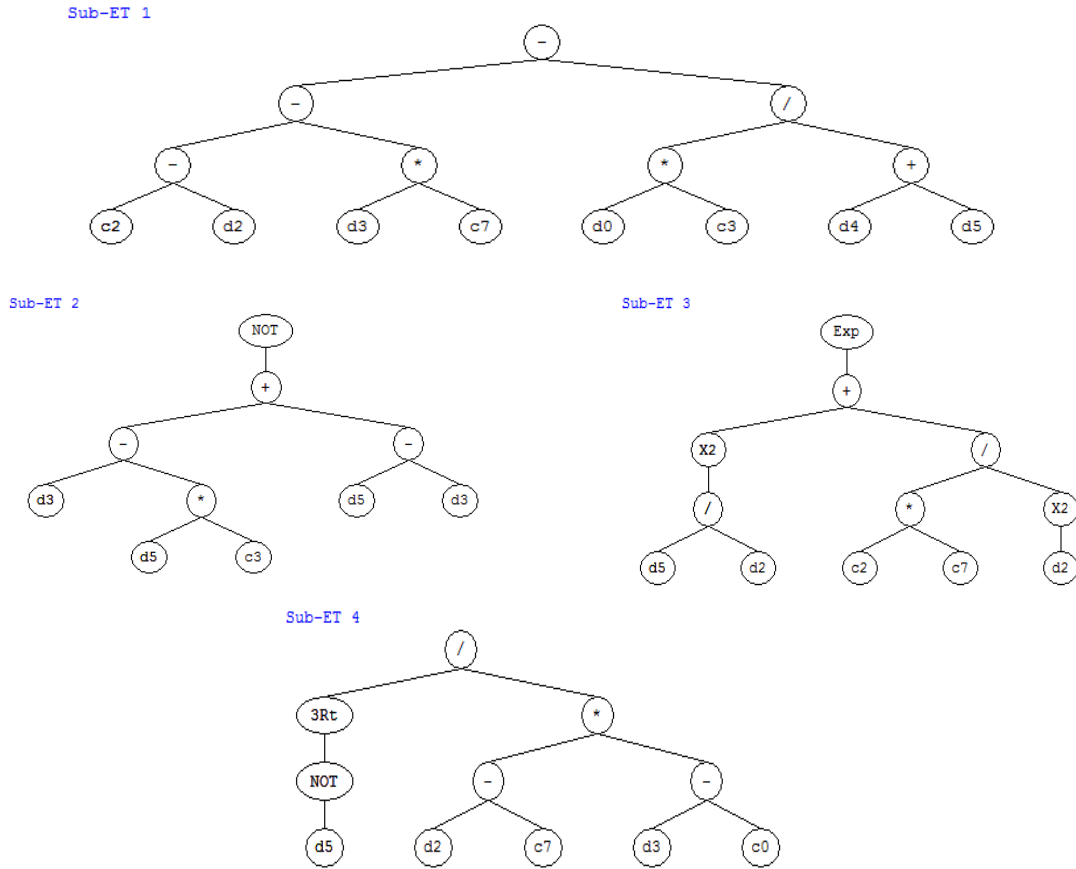


Figure 4. Expression tree for predicting the remaining pyrite fraction.

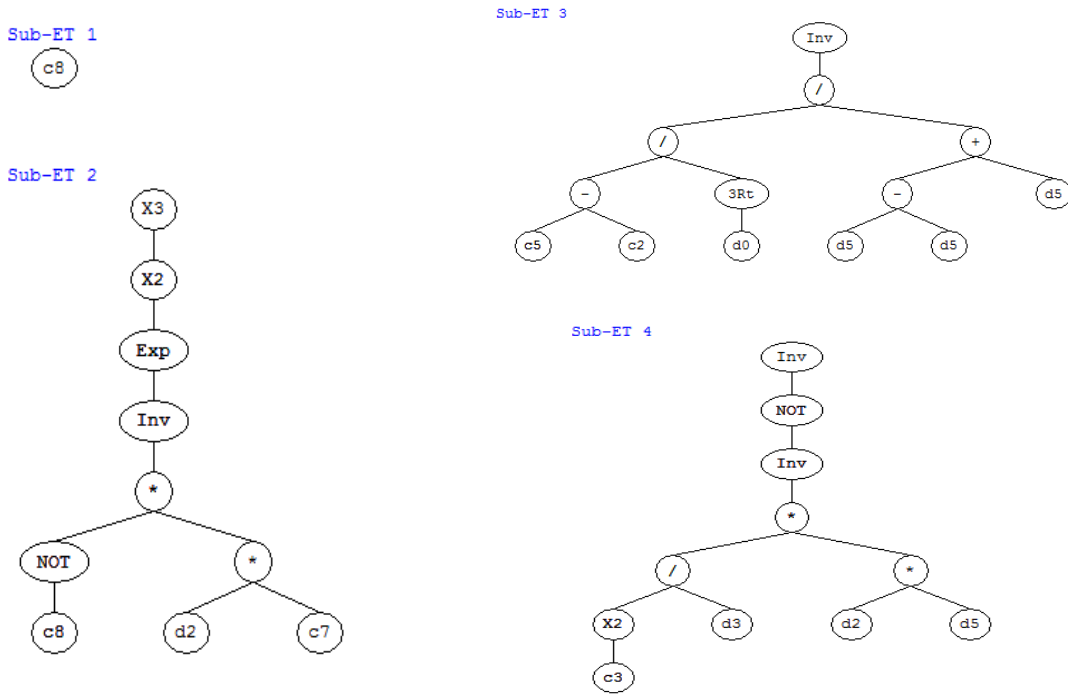


Figure 5. Expression tree for predicting the remaining chalcopyrite fraction.

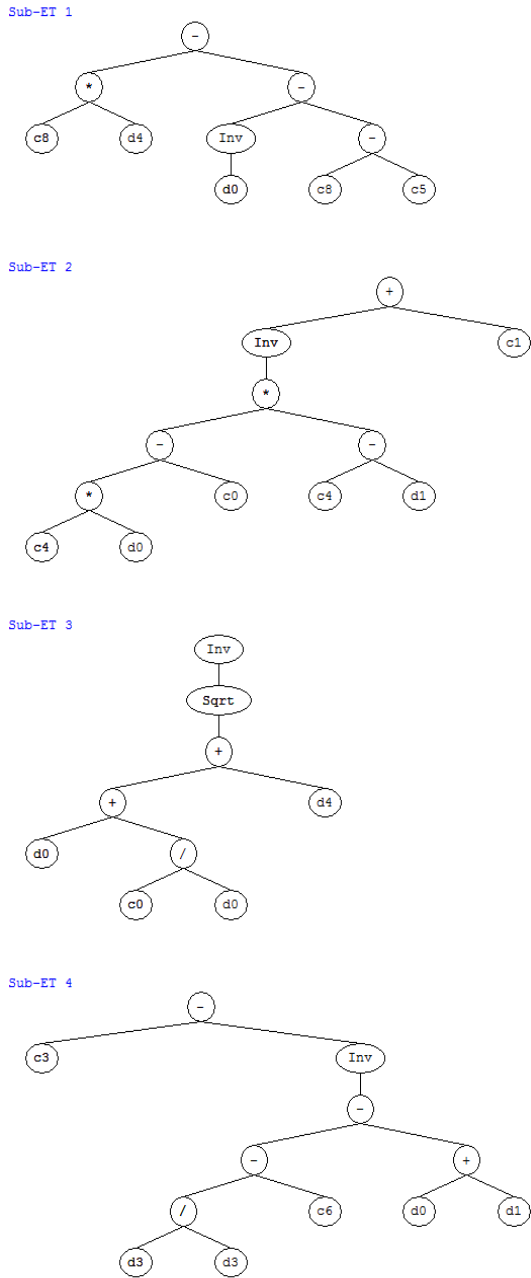


Figure 6. Expression tree for predicting the sulfate content.

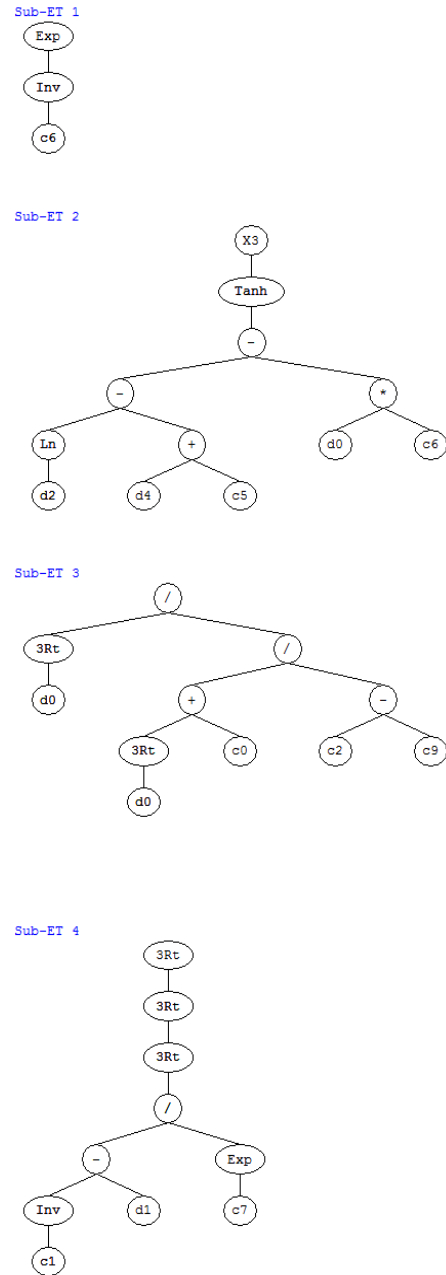


Figure 7. Expression tree for predicting the pH values.

Equations (7)-(10) show the suggested relationships developed using the GEP algorithm for predicting the remaining pyrite fraction, remaining chalcopyrite fraction, sulfate content, and pH, respectively.

For validation of the suggested relationships of GEP, the results obtained were compared using the coefficient of determination (R^2) and root-mean-

square error (RMSE) in order to find the best model for each one of the output parameters (Table 5). Figures 8-11 show the validation diagrams for different output parameters. Figure 10 demonstrates the identified relationships between the measured data and the predicted data for the output parameters.

$$\begin{aligned}
 Py = & \left(((-9.86449 - CL) - (N \times 6.25204)) - (D \times 5.95461) \div (NN + IPy) \right) \\
 & \times \left(1 - \left((N - (IPy \times 4.15766)) + (IPy - N) \right) \right) \\
 & \times \left(\exp \left(\left(\frac{IPy}{CL} \right)^2 - \frac{60.66362}{CL^2} \right) \right) \times \left(\frac{\sqrt[3]{1 - IPy}}{(CL - 1.60375) \times (N + 7.85827)} \right)
 \end{aligned} \tag{7}$$

$$ChPy = 3.00332 \times \left(\exp \left(\frac{1}{-0.54748 \times CL} \right) \right)^5 \times \left(\frac{IChPy \times \sqrt[3]{D}}{5.69108} \right) \times \left(\frac{1}{1 - \frac{1}{\frac{75.25059}{N} \times (CL \times IChPy)}} \right) \tag{8}$$

$$\begin{aligned}
 S = & \left((7.06495 \times NN) - \left(\frac{1}{D} - 16.54812 \right) \right) \\
 & \times \left(\frac{1}{\left((-1.30340 \times D) + 1.24146 \right) \times (-1.30340 - Bi) - 9.89024} \right) \\
 & \times \left(\frac{1}{\sqrt{D + \frac{1.61168}{D} + NN}} \right) \times \left(-4.59823 - \frac{1}{11.88665 - (D + Bi)} \right)
 \end{aligned} \tag{9}$$

$$\begin{aligned}
 pH = & \left(\exp \frac{1}{0.45182} \right) \times \left(\tanh \left((\ln CL - (NN + 8.79182)) + (0.88256 \times D) \right) \right)^3 \\
 & \times \left(\frac{\sqrt[3]{D} \times 4.12122}{\sqrt[3]{D} + 7.79103} \right) \times \sqrt[27]{\frac{-0.09363 - Bi}{\exp(-4.77258)}}
 \end{aligned} \tag{10}$$

Table 5. GEP results.

Parameter		Value			
		Py	Chpy	S	pH
Training	RMSE	0.1415	0.0154	121.8109	0.5556
	R-square	0.936	0.917	0.891	0.915
Validation	RMSE	0.1409	0.0147	150.3013	0.5435
	R-square	0.921	0.91	0.861	0.888



Figure 8. Cross-plot of model results versus measured data for data validation on the remaining pyrite fraction.



Figure 9. Cross-plot of model results versus measured data for data validation on the remaining chalcopyrite fraction.

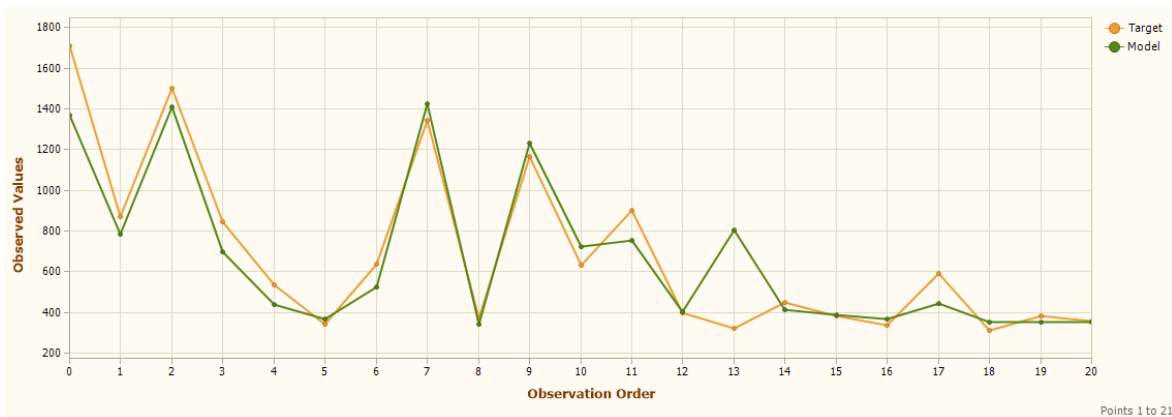


Figure 10. Cross-plot of model results versus measured data for data validation on the sulfate content.

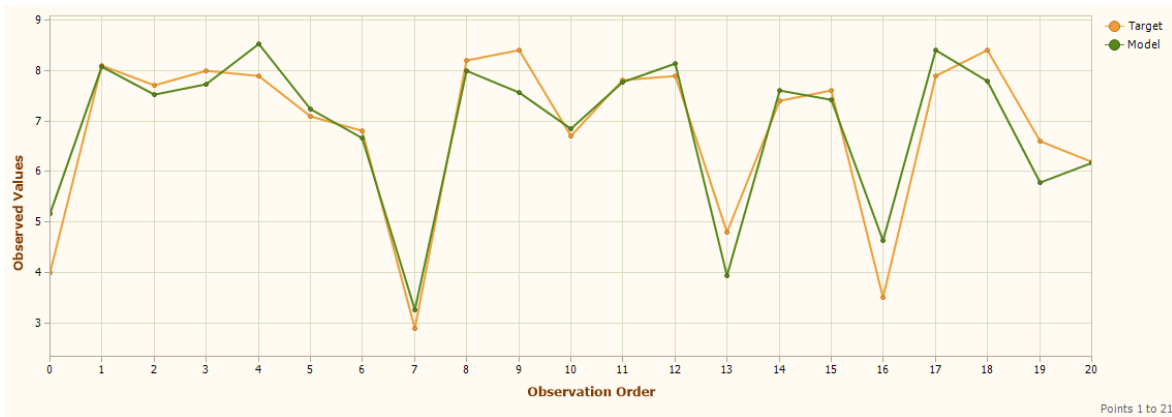


Figure 11. Cross-plot of model results versus measured data for data validation on the pH value.

Figures 12 and 13 demonstrate the identified relationships between the measured data and the predicted data for the output parameters. The coefficients of determination for the remaining pyrite fraction, remaining chalcopyrite fraction, sulfate, and pH were 0.92, 0.91, 0.86, and 0.89,

respectively. Due to the high values of the correlations between the predicted data and the measured data, it seems that GEP could predict the output parameters, and could be applied in similar cases.

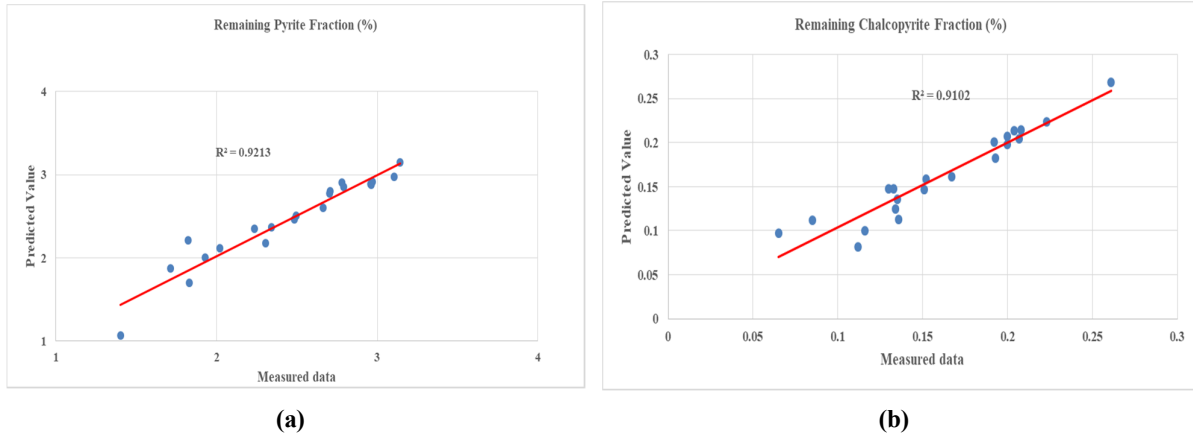


Figure 12. Relationship between the predicted data and the measured data for a) the remaining pyrite fraction and b) the remaining chalcopyrite fraction.

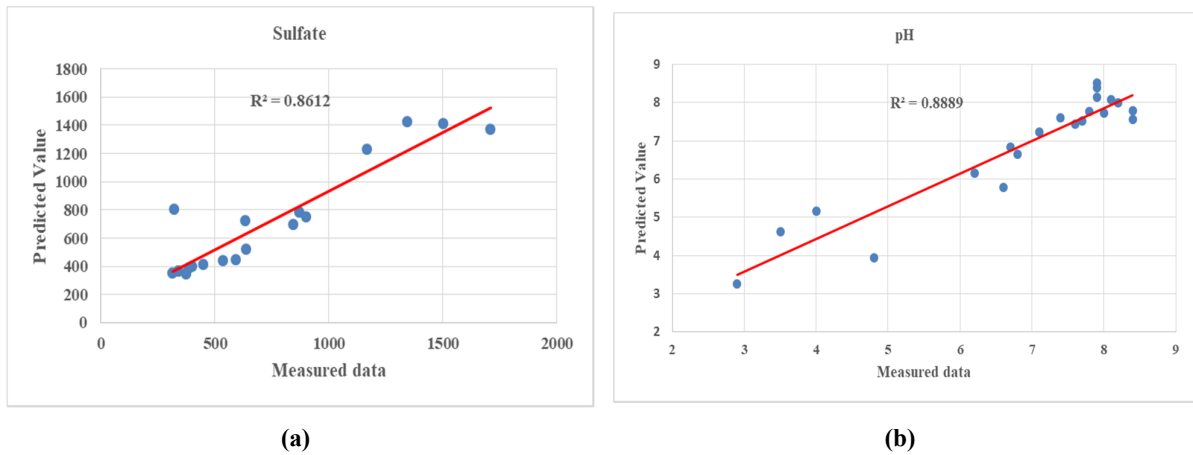


Figure 13. Relationship between the predicted data and the measured data for a) sulfate and b) pH values.

4. Conclusions

The GEP algorithm was applied in order to suggest four relationships in the AMD generation process based on the pyrite and chalcopyrite oxidation process in copper tailing particles. For this, a dataset including 70 actual data was built. Then it was divided into the training data including 30% of data, and the rest of the data was applied as the validation set for evaluating the GEP prediction. Then using the GEP algorithm, three empirical relationships were proposed for predicting the remaining pyrite fraction, remaining chalcopyrite fraction, sulfate content, and pH values based on the tailings depth, concentrations of bicarbonate, chloride, nitrate, nitrite, and initial pyrite and chalcopyrite fractions. Accordingly, RMSE of the validation models was calculated as 0.1409, 0.0147, 150.301, and 0.5435 for the pyrite, chalcopyrite, and sulfate concentrations, and pH value, respectively, associated with 0.92, 0.91, 0.86, and 0.89, respectively. The low value of

RMSE and high values of coefficients of the determination indicated an appropriate estimation of the parameters affecting the oxidation process of sulfide minerals and AMD production. Also other techniques such as the multiple linear regression and other AI techniques such as ANNs or GP could be applied for a better evaluation of the GEP results.

5. Disclosure of potential conflicts of interest

The authors declare that they have no conflict of interest. Also they declare that they did not receive any funds for carrying out this research work.

6. References

[1]. Blowes, DW., Ptacek, CJ., Jambor, JL., Weisener, CG., Paktunc, D., Gould, WD. and Johnson, DB. (2003). The geochemistry of acid mine drainage. 10.1016/B978-0-08-095975-7.00905-0

- [2]. Buckley, AN. and Woods, RW. (1987). The surface oxidation of pyrite. *Applied Surface Science*, 27: 437–452.
- [3]. Brown, AD. and Jurinak, JJ. (1989). Pyrite oxidation in aqueous mixtures. *Journal of Environmental Quality* 18: 545–550.
- [4]. Wiersma, CL. and Rimstidt, JD. (1984). Rates of reaction of pyrite and marcasite with ferric iron at pH 2. *Geochimica et Cosmochimica Acta* 48: 85–92.
- [5]. Sasaki, K., Tsunekawa, M., Ohtsuka, T. and Konno, H. (1995). Confirmation of a sulfur-rich layer on pyrite after oxidative dissolution by Fe(III) ions around pH 2. *Geochimica et Cosmochimica Acta* 59: 3155–3158.
- [6]. Rimstidt, JD., Chermak, JA. and Gagen, PM., (1994). Rates of reaction of galena, sphalerite, chalcopyrite and arsenopyrite. In: Alpers CN and Blowes DW (eds.) *Environmental Geochemistry of Sulfide Oxidation*, vol. 550, pp. 2–13. Washington, DC: American Chemical Society.
- [7]. Ferguson K.D. and Erickson P.M., (1988). Pre-Mine Prediction of Acid Mine Drainage. In: Salomons W., Förstner U. (eds) *Environmental Management of Solid Waste*. Springer, Berlin, Heidelberg.
- [8]. Rooki, R., Doulati Ardejani, F., Aryafar, A. and Asadi, AB. (2011). Prediction of heavy metals in acid mine drainage using artificial neural network from the Shur River of the Sarcheshmeh porphyry copper mine, Southeast Iran. *Environmental Earth Sciences*. 64 (5): 1303-1316.
- [9]. Aryafar, A., Gholami, R., Rooki, R. and Doulati Ardejani, F. (2012). Heavy metal pollution assessment using support vector machine in the Shur River, Sarcheshmeh copper mine, Iran. *Environmental Earth sciences*, 67(4): 1191-1199.
- [10]. Doulati Ardejani, F., Rooki, R., Jodieri Shokri, B., Eslam Kish, T., Aryafar, A. and Tourani, P. (2012). Prediction of rare earth elements in neutral alkaline mine drainage from Razi coal mine, Golestan Province, northeast Iran, using general regression neural network. *Journal of Environmental Engineering*. 139 (6): 896-907.
- [11]. Sadeghiamirshahidi, M. and Doulati Ardejani, F., (2013). Application of artificial neural networks to predict pyrite oxidation in a coal washing refuse pile. *Fuel*, 104: 163-169.
- [12]. Bouzazhah, H., Benzaazoua, M. and Bussiere, B. (2014). Prediction of Acid Mine Drainage: Importance of Mineralogy and the Test Protocols for Static and Kinetic Tests. *Mine Water and the Environment* 33: 54–65.
- [13]. Jodeiri Shokri, B., Ramazi, H., Doulati Ardejani, F. and Sadeghiamirshahidi, M. (2014). Prediction of pyrite oxidation in a coal washing waste pile applying artificial neural networks (ANNs) and adaptive neuro-fuzzy inference systems (ANFIS). *Mine Water and the Environment*. 33 (2): 146-156.
- [14]. Jodeiri Shokri, B., Ramazi, H., Doulati Ardejani, F. and Moradzadeh, A. (2014). A statistical model to relate pyrite oxidation and oxygen transport within a coal waste pile: case study, Alborz Sharghi, northeast of Iran. *Environmental Earth sciences*. 71 (11): 4693-4702.
- [15]. Bahrami, S. and Doulati Ardejani, F. (2016). Prediction of pyrite oxidation in a coal washing waste pile using a hybrid method, coupling artificial neural networks and simulated annealing (ANN/SA). *Journal of Cleaner Production*, 137: 1129-1137.
- [16]. Dold, Bernhard. (2017). Acid rock drainage prediction: A critical review. *Journal of Geochemical Exploration* 172: 120-132.
- [17]. Balci, N. and Demirel, C. (2018). Prediction of acid mine drainage (AMD) and metal release sources at the Küre Copper Mine Site, Kastamonu, NW Turkey. *Mine Water and the Environment*. 37 (1): 56-74.
- [18]. Hadadi, F., Jodeiri Shokri, B, Zare Naghadehi, M., Doulati Ardejani, F., (2020). Probabilistic prediction of acid mine drainage generation risk based on pyrite oxidation process in coal washery rejects-A Case Study. *Journal of Mining and Environment*. 10.22044/jme.2020.9609.1873
- [19]. Sebogodi, KR., Johakimu, JK., B. and Sithole, B. (2020). Beneficiation of pulp mill waste green liquor dregs: Applications in treatment of acid mine drainage as new disposal solution in South Africa. *Journal of Cleaner Production* 246: 118979.
- [20]. Luis, P, Beltran, L., Scharwz, A., Cristina Ruiz, M. and Borquez, R. (2020). Optimization of nanofiltration for treatment of acid mine drainage and copper recovery by solvent extraction. *Hydrometallurgy*, 195: 105361
- [21]. Zhou, Y., Zhou, W., Lu, X., Jiskani, IM., Cai, Q., Liu, P. and Li, L. (2020). Evaluation Index System of Green Surface Mining in China. *Mining, Metallurgy & Exploration* 37: 1093–1103.
- [22]. Chen, J., Jiskani IM., Jinliang, C. and Yan H. (2020). Evaluation and future framework of green mine construction in China based on the DPSIR model. *Sustainable Environment Research*. 30 (1): 1-10.
- [23]. Behnia, D. and Shahriar, K. (2015). Prediction of Tunnelling-induced Settlement Using Gene Expression Programming. *American Rock Mechanics Association. 49th U.S. Rock Mechanics/Geomechanics Symposium*, 28 June-1 July, San Francisco, California.
- [24]. Johari, A., Hooshm and Nejad, A. (2015). Prediction of soil-water characteristic curve using gene expression programming. *IJST, Transactions of Civil Engineering*, 39, 143-165.
- [25]. Shirani Faradonbeh, R., Hasanipanah, M., Amnieh, H.B., Armaghani, D.J. and Monjezi, M. (2018). Development of GP and GEP models to estimate

an environmental issue induced by blasting operation. Environmental Monitoring and Assessments, 190,351.

[26]. Thneibat, M. and Tarawneh, B. (2019). Genetic expression programming model for selecting the appropriate ground improvement technique. Journal of Engineering and Applied Sciences. 14 (20): 3469-3480.

[27]. Hajihassani, M., Abdullah, S.S., Asteris, P.G. and Armaghani, D.J. (2019) A Gene Expression Programming Model for Predicting Tunnel Convergence. Appl. Sci, 9, 4650.

[28]. Jannesar Malakooti, S., Shafaei Tonkaboni., SZ. Noaparast, M., Doulati Ardejani, F. and Naseh, R. (2014) Characterization of the Sarcheshmeh copper mine tailings, Kerman province, southeast of Iran. Environmental Earth Sciences., 71: 2267-2291.

[29]. Ferreira, C. (2001). Gene expression programming: a new adaptive algorithm for solving problems. arXiv preprint cs/0102027.

[30]. Ferreira, C. (2006). Gene expression programming: mathematical modelling by an artificial intelligence (Vol. 21). pp. 55-56. Springer.

پیش‌بینی پتانسیل تولید زهاب اسیدی معدن از ذرات باطله‌های مس با استفاده از الگوریتم بیان ژن - مطالعه موردی

بهشاد جدیری شگری^{۱*}، حسام دهقانی^۱، رضا شمسی^۱ و فرامرز دولتی ارده جانی^۲

۱- گروه مهندسی معدن، دانشگاه صنعتی همدان، همدان، ایران

۲- دانشکده مهندسی معدن، پردیس دانشکده‌های فنی دانشگاه تهران، تهران، ایران

ارسال ۲۰۲۰/۰۸/۳۱، پذیرش ۲۰۲۰/۱۱/۰۲

* نویسنده مسئول مکاتبات: b.jodeiri@hut.ac.ir

چکیده:

در این تحقیق، یک روش کمی پیش‌بینی احتمال فرآیند تولید زهاب اسیدی معدن در ذرات باطله‌های ناشی از معدن مس سرچشمه که در جنوب ایران قرار دارد، ارائه شده است. در حقیقت، چهار رابطه برای پیش‌بینی، میزان پیریت باقی‌مانده، میزان کالکوپیریت باقی‌مانده، غلظت سولفات و اسیدیته با استفاده از روش الگوریتم بیان ژن، پیشنهاد شده‌اند. برای نیل به این هدف، پس از گردآوری یک پایگاه داده‌ای مناسب، برخی از با اهمیت ترین پارامترها مانند عمق قرارگیری ذرات باطله، میزان پیریت اولیه، کالکوپیریت اولیه و نیز غلظت‌های بی‌کربنات، نیتريت، نیترات و کلراید، بعنوان داده‌های ورودی در نظر گرفته شدند. سپس، ۳۰ درصد از داده‌های ورودی بصورت تصادفی جهت آموزش داده‌ها انتخاب شدند، در حالیکه داده‌های اعتبارسنجی، شامل ۷۰ درصد باقی‌مانده پایگاه داده‌ها بودند. در ادامه، روابط با استفاده از روش بیان ژن پیشنهاد شدند. مقادیر بالای ضرایب تعیین (۰/۹۲، ۰/۹۱، ۰/۸۶ و ۰/۸۹) و نیز میزان کم مقادیر مجذور میانگین مربع خطاها (۰/۱۴۰، ۰/۱۴، ۰/۱۴ و ۰/۱۴) در تعیین میزان پیریت باقی‌مانده، میزان کالکوپیریت باقی‌مانده، غلظت سولفات و اسیدیته، حاکی از آن است که اعتبارسنجی این روابط بخوبی انجام شده است. نتایج بدست آمده نشان دادند که روش الگوریتم بیان ژن می‌تواند بعنوان یک روش نوآور جدید در پیش‌بینی فرآیند تشکیل زهاب اسیدی معدن بکار گرفته شود.

کلمات کلیدی: زهاب اسیدی معدن، باطله‌های مس، پیریت، کالکوپیریت، برنامه نویسی بیان ژن.